Conf-780486--1

CREEP-FATIGUE INTERACTIONS IN AN AUSTENITIC STAINLESS STEEL

S. Majumdar and P. S. Maiya

prepared for

2nd Canadian Fracture Conference
on Temperature and Environmental Effects on Failure
University of Waterloo
Waterloo, Ontario, Canada
April 21, 1978

U of C-AUA-USDOE

ARGONNE NATIONAL LABORATORY, ARGONNE, ILLINOIS

Operated under Contract W-31-109-Eng-38 for the U. S. DEPARTMENT OF ENERGY

Creep-fatigue Interactions in an Austenitic Stainless Steel*

by

S. Majumdar and P. S. Maiya

Materials Science Division
ARGONNE NATIONAL LABORATORY
Argonne, Illinois 60439

ABSTRACT

A phenomenological model of the interaction between creep and fatigue in Type 304 stainless steel at elevated temperatures is presented. The model is based on a crack-growth equation and an equation governing cavity growth, expressed in terms of current plastic strain and plastic strain rate. Failure is assumed to occur when a proposed interaction equation is satisfied. Various parameters of the equations can be obtained by correlation with continuously cycling fatigue and monotonic creep-rupture test data, without the use of any hold-time fatigue tests. Effects of various wave shapes such as tensile, compressive, and symmetrical hold on the low-cycle fatigue life can be computed by integrating the damage-rate equations along the appropriate loading path. Microstructural evidence in support of the proposed model is also discussed.

---

*Work supported by the U.S. Department of Energy.

Creep-fatigue Interactions in an Austenitic Stainless Steel*

by

S. Majumdar and P. S. Maiya

Materials Science Division
ARGONNE NATIONAL LABORATORY
Argonne, Illinois 60439

Introduction

Low-cycle fatigue at elevated temperatures is an important consideration in the design and operation of structural components for many nuclear and non-nuclear applications. Fatigue failure can occur by fatigue and/or interactions between creep and fatigue, depending on the loading-wave shape. Initially, some investigators [1,2] attributed the effects of wave shape entirely to the test environment. However, additional experiments [3-5] conducted on materials such as Type 304 stainless steel suggest that wave-shape effects are important both in air and in vacuum. Extensive low-cycle fatigue testing at elevated temperatures has demonstrated that in Type 304 stainless steel, hold times in tension either at constant total strain or stress have more severe deteriorating effects on fatigue life than hold times in compression or symmetrical hold cycles involving equal hold times in tension and compression [6,7]. The damaging effects associated with hold times are also reflected in the fracture modes of specimens. For example, the fractures observed in specimens tested under compressive and symmetric hold times are transgranular with striated fracture surfaces, whereas, in general, the specimens tested under tensile hold fail in an intergranular manner [8,9], which is associated with grain-boundary cavity initiation

---

*Work supported by the U.S. Department of Energy.

and growth [10]. Recently, Tomkins and Wareing [11] have proposed a model of elevated-temperature fatigue that involves interaction between a crack propagating from the surface of the specimen and cavities in the bulk of the material. A theory of creep-fatigue interaction that considers the initiation of grain-boundary cavities has also been proposed by Raj [12]. The present paper describes a damage-rate approach which is a generalization of an earlier creep-fatigue interaction model presented elsewhere by the authors [13]. In particular, the present approach considers two types of damage, "crack damage" and "cavity damage," which are assumed to accumulate in the material independent of each other. Failure in the material occurs when a proposed interaction equation is satisfied. It will be shown that the above procedure enables one to take into account the effects of various wave shapes on the low-cycle fatigue life.

To demonstrate the applicability of the generalized approach to a variety of wave shapes, three types of tests were conducted on Type 304 stainless steel at 593°C (1100°F). The first type (slow-fast) involved a slow tensile strain rate followed by a fast compressive strain rate without any hold time. Secondly, tests were run with a fast tensile strain rate followed by a slow compressive strain rate without any hold time (fast-slow). Finally, several tests were conducted in which hold times in tension and compression per cycle were not equal. The fracture surfaces were examined by means of scanning-electron microscopy. The fatigue data are compared with the large amount of fatigue data available for the same heat of material under more conventional modes of loading, and the results are evaluated in terms of the damage-rate approach.

Damage-rate Approach

We assume that a characteristic crack length, a, and cavity size, c, determine the extent of accumulated damage, and that failure of a low-cycle

fatigue specimen occurs as a result of the growth of preexisting cracks and cavities of initial sizes a_o and c_o, respectively. The rate of growth of cracks and cavities is assumed to be governed by the following equations:

$$\frac{1}{a}\frac{da}{dt} = \begin{cases} T|\varepsilon_p|^m|\dot{\varepsilon}_p|^k & \text{for tension} \\ C|\varepsilon_p|^m|\dot{\varepsilon}_p|^k & \text{for compression} \end{cases} \tag{1}$$

and

$$\frac{1}{c}\frac{dc}{dt} = \begin{cases} G|\varepsilon_p|^m|\dot{\varepsilon}_p|^{k_c} & \text{for tension} \\ -G|\varepsilon_p|^m|\dot{\varepsilon}_p|^{k_c} & \text{for compression} \end{cases} \tag{2}$$

where $|\varepsilon_p|$ and $|\dot{\varepsilon}_p|$ represent the current absolute values of plastic strain and strain rate, respectively. The material parameters T, C, G, m, k, and k_c are functions of temperature, microstructure, and environment. It is assumed that the incremental cavity damage can be negative and that any cavity of size $\leq c_o$ anneals out immediately; thus, the net calculated cavity size (c) is not allowed to be less than the initial cavity size (c_o). It should be noted that although stress does not appear explicitly in Eqs. (1) and (2), it is implicitly involved because the plastic strain and plastic strain rate can be related to the stress if one assumes an equation-of-state theory similar to that proposed by Hart [14]. Ideally, a material structural-state variable instead of plastic strain should be used in Eqs. (1) and (2). However, for the loading cases considered in the present paper, the plastic strain reflects the material structural-state variable.

To compute fatigue life, a knowledge of the interaction between the crack and the cavities is required. While this is an unsolved problem, we

have assumed that the following interaction equation governs the failure of the low-cycle fatigue specimen:

$$\frac{\ell n\ a/a_o}{\ell n\ a_f/a_o} + \frac{\ell n\ c/c_o}{\ell n\ c_f/c_o} = 1 \tag{3}$$

where a_f is the final crack size in a specimen free of cavities, and c_f is the final cavity size in a specimen free of cracks and is thus related to cavity spacing. However, when the present method is used to predict low-cycle fatigue lives of hourglass specimens of identical size and microstructure, exact values of a_o, a_f, c_o, and c_f will not be required. The damage-rate equations (1) and (2) can be integrated along various loading paths to estimate the cavity and crack damage; by means of the interaction equation (3), the continuous-cycling fatigue life (N_f) or time to failure (t_R) can then be obtained [15] as follows:

$$N_f = \frac{m+1}{4A}\left(\frac{\Delta\epsilon_p}{2}\right)^{-(m+1)} \dot{\epsilon}_p^{\,1-k}, \tag{4}$$

where $$A = \frac{T+C}{2} \Big/ \ell n\ \frac{a_f}{a_o},$$

$\Delta\epsilon_p$ = plastic strain range,

and $\dot{\epsilon}_p$ = plastic strain rate.

The monotonic creep rupture is given by

$$t_R = \left(\frac{m+1}{f_1 + f_2}\right)^{\frac{1}{m+1}} \dot{\varepsilon}_p^{-\left(\frac{k_c+m}{1+m}\right)} \tag{5}$$

where $f_1 = (T'/\ell n\ a_f/a_o)\dot{\varepsilon}_p^{k-k_c}$

and $f_2 = G'/\ell n\ c_f/c_o$.

For creep tests at low stress, cavity damage predominates over crack damage ($f_2 >> f_1$) so that

$$t_R \propto \dot{\varepsilon}_p^{-\frac{k_c+m}{1+m}} .$$

For fast-slow saw-tooth waveform tests,

$$N_f = \frac{m+1}{4A}\left(\frac{\Delta\varepsilon_p}{2}\right)^{-(m+1)} \left[\frac{\dot{\varepsilon}_f^{k-1}}{1 + C/T} + \frac{\dot{\varepsilon}_s^{k-1}}{1 + T/C}\right]^{-1} . \tag{6}$$

where $\dot{\varepsilon}_f$ = fast tensile strain rate

and $\dot{\varepsilon}_s$ = slow compressive strain rate.

The cavity damage for this case is zero. For slow-fast saw-tooth waveform tests,

$$N_f = \left\{ \frac{4A}{m+1} \left(\frac{\Delta\varepsilon_p}{2} \right)^{m+1} \left[\frac{\dot{\varepsilon}_s^{\,k-1}}{1 + C/T} + \frac{\dot{\varepsilon}_f^{\,k-1}}{1 + T/C} \right] \right.$$

$$\left. + \frac{C_g}{m+1} \left(\frac{\Delta\varepsilon_p}{2} \right)^{m+1} \left[\dot{\varepsilon}_s^{\,k_c-1} - \dot{\varepsilon}_f^{\,k_c-1} \right] \right\}^{-1} \qquad (7)$$

where $C_g = G/\ln(c_f/c_o)$,

$\dot{\varepsilon}_s$ = slow tensile strain rate,

and $\dot{\varepsilon}_f$ = fast compressive strain rate.

For hold-time fatigue tests,

$$N_f = 1/(d_T + d_C) \qquad (8)$$

where d_T and d_C are the crack and cavity damage per cycle, respectively, and are expressed as:

$$d_T = \frac{4A}{m+1} \left(\frac{\Delta\varepsilon_p}{2} \right)^{m+1} \dot{\varepsilon}_p^{\,k-1} + \frac{2A}{1 + C/T} \int_o^{t_t} |\varepsilon_p|^m |\dot{\varepsilon}_p|^k \, dt$$

$$+ \frac{2A}{1 + T/C} \int_o^{t_c} |\varepsilon_p|^m |\dot{\varepsilon}_p|^k \, dt \, ,$$

$$d_C = C_g \int_o^{t_t} |\varepsilon_p|^m |\dot{\varepsilon}_p|^{k_c} \, dt - C_g \int_o^{t_c} |\varepsilon_p|^m |\dot{\varepsilon}_p|^{k_c} \, dt \, , \qquad (10)$$

and t_t and t_c are the hold times in tension and compression, respectively.

Experimental Procedure

Low-cycle fatigue tests were performed on hourglass-shape specimens (6.35-mm minimum diameter) of Type 304 stainless steel (heat 9T2796). The chemical composition of this steel has been reported elsewhere [8]. Prior to fatigue tests, all specimens were solution annealed in evacuated quartz tubes back-filled with argon for 1/2 h at 1092°C, and aged for 1000 h at 593°C. The experiments were conducted at a temperature of 593°C in air under push-pull conditions in an axial strain-control mode, using a procedure similar to that outlined by Slot et al. [15]. Essentially, the tests involved two types of waveforms: (1) saw-tooth waveform and (2) cyclic relaxation with unequal hold times in tension and compression. After fatigue failure (complete separation), the fracture surfaces were examined by scanning-electron microscopy to establish the predominant mode of fracture. In addition, surfaces near and perpendicular to the fracture surface of a few specimens were prepared for examination of grain-boundary cavities caused by grain-boundary sliding. The specimens were mounted in Bakelite and carefully ground on silicon carbide papers (400 and 600 grit), using water as a lubricant. Coarser silicon carbide papers were avoided to minimize surface damage that might result in closure of cavities. Metallographic polishing was carried out in a conventional manner on cloth impregnated with a suspension of 0.3-μm Al_2O_3 in water; final polishing was performed with 0.05-μm Al_2O_3. The polished specimens were examined by optical and scanning-electron microscopy.

Results and Discussion

The total ($\Delta\varepsilon_t$) and plastic ($\Delta\varepsilon_p$) strain ranges and saturation stress range ($\Delta\sigma_s$) obtained at approximately half the life, strain rate ($\dot{\varepsilon}_t$), cycles to failure (N_f), and other experimental parameters for all the tests involving saw-tooth waveforms and unsymmetrical hold times are listed in Table I. It should be pointed out that in the slow-fast and fast-slow tests, virtually no mean stress was developed [15]. Table I shows that slow-fast loading reduces life significantly compared to fast-fast and fast-slow loadings. Similar results also have been reported by Coffin [4]. The effects of waveshape on fracture mode are illustrated in Figs. 1 and 2, which show the scanning-electron micrographs of the fracture surfaces of the specimens subjected to saw-tooth and symmetrical waveforms. For the loading cases in which the tensile strain rate is greater than or equal to the compressive strain rate, the fracture mode is transgranular with well-defined striations occurring on the fracture surface (Figs. 1a, b, c and 2a, b, c). On the other hand, slow-fast loading produces an intergranular fracture mode (Figs. 1d and 2d), even when the "slow" strain rate is as high as 10^{-4}/s. This observation suggests that the fracture mode is more strongly influenced by the effects of the initiation and growth of grain-boundary cavities during the long tensile part of the cycle than by the effects of the shrinkage of cavities during the short compressive part of the cycle. The intergranular fracture in slow-fast tests occurs by grain-boundary cavitation; an example of this is shown in Fig. 3. Such cavities are not observed for either the fast-slow or the symmetrical-loading case. Figure 3 also shows that the damage was more pronounced in the boundary normal to the direction of stress than in the other boundaries.

If tensile hold favors grain-boundary cavity initiation and growth and compressive hold promotes cavity shrinkage, one would expect that longer tensile hold times, followed in each instance by a short compressive hold, would be far less damaging than tensile hold alone. The results obtained from unsymmetrical hold-time tests (Table I) are consistent with the above idea. When a 15-min tensile hold time and 5-min compressive hold time are present in each cycle, predominantly transgranular fracture occurs [15]. A specimen subjected to completely symmetrical hold time with the same period as the unsymmetrical hold has an even longer life because of the more complete annealing-out of cavities. The fracture mode in the case of symmetrical hold time is also transgranular. Cavity growth during tensile hold and shrinkage during compressive hold also play an important role in hold-time-sequence fatigue experiments performed on Type 304 stainless steel [16].

The generalized damage-rate approach can be used to predict fatigue life, provided the various material parameters A, k, m, T/C, k_c, and C_g [see Eqs. (9) and (10)] are known. The values of parameters A, k, and m have been obtained from a least-squares fit of symmetrical continuous-cycling fatigue data [13] to Eq. (4). The ratio T/C is assumed to be equal to 4 [18]; it can also be obtained from Eq. (6). The exponent k_c was determined by equating the slope of the log-log plot of time to stress-rupture versus minimum creep rate (Fig. 4) to the exponent in Eq. (5). Thus, no hold-time data were used to determine any of the parameters tabulated in Fig. 5. It is interesting to note that if the time to monotonic creep rupture is calculated for Type 304 stainless steel using Eq. (5) and assuming $T' = T$ and $G' = G$, one obtains the dotted line shown in Fig. 4. Thus it appears that for this material, satisfactory estimates of the parameter C_g may be obtained by correlation of creep-rupture data with Eq. (5). The creep-fatigue life prediction based on Eqs. (9) and (10) assumes a knowledge of plastic strain rate

during hold time. This was obtained from the stress relaxation behavior, which can be described by:

$$\ell n \frac{\sigma_i}{\sigma} = \frac{B}{1 + p} t^{1 + p} \qquad (11)$$

where σ_i is the stress at the beginning of relaxation, and B and p are parameters that were determined for each test (at half-life) by a least-squares fit. These parameters are listed in Table II. A comparison of predicted versus experimental life for tests involving saw-tooth waveforms and unsymmetrical hold times is shown in Fig. 5. For the purpose of comparison, data from more conventional hold-time tests are also included; T, S, and C refer to tensile, symmetrical, and compressive hold, respectively. In addition, Fig. 5 shows fatigue-test results obtained at 482° and 538°C. In most cases, the predicted life is within a factor of two (dashed line) of the experimentally observed life. It should be noted that the same "cavity damage" parameters (C_g and k_c) are used at all temperatures. The difference in the calculated lives at different temperatures arises from the effect of temperature on the stress-relaxation rate of the material. The relative insensitivity of the parameters C_g and k_c to temperature in the range 482 to 593°C suggests that cavity damage in this temperature range is not a diffusion-controlled process but dependent on the plastic strain and strain rate (i.e., the amount of grain-boundary sliding) during hold times. It is interesting to note that a similar conclusion has been reported for nickel in high-temperature creep studies [19].

Conclusions

High-temperature fatigue results for Type 304 stainless steel obtained from tests that involve unequal ramp rates and unequal hold times in tension

and compression are presented. The effects of various waveshapes on fracture mode are discussed. When the tensile strain rate is slower than the compressive strain rate, intergranular fracture occurs as a result of grain-boundary cavity initiation and growth. Imposition of short compressive hold times in addition to tensile hold times significantly lengthens the fatigue life of Type 304 stainless steel.

These microstructural observations are reflected in the development of a generalized damage-rate approach which considers two major types of damage mechanisms, one associated with crack initiation and growth and another with grain-boundary cavity initiation and growth. The effects of various wave shapes on fatigue life can be predicted by means of an assumed interaction equation between the two modes of damage.

References

[1] Coffin, L. F., Jr., "The Effect of HIgh Vacuum on the Low-cycle Fatigue Law," Metallurgical Transactions, Vol. 3, No. 7, 1972, pp. 1777-1788.

[2] Achter, M. R., "Effect of Environment on Fatigue Cracks," in *Fatigue Crack Propagation*, ASTM STP 415 (American Society for Testing and Materials, Philadelphia, 1967), pp. 181-202.

[3] Sheffler, K. D. and Doble, G. S., "Thermal Fatigue Behavior of T-111 and Astar 811-C in Ultrahigh Vacuum," in *Fatigue at Elevated Temperatures*, ASTM STP 520 (American Society for Testing and Materials, Philadelphia, 1973), pp. 491-499.

[4] Coffin, L. F., Jr., "Observations and Correlations Emphasizing Frequency and Environmental Effects," in *Time-Dependent Fatigue of Structural Alloys*, ORNL-5073 (Oak Ridge National Laboratory, January 1977), p. 101.

[5] P. S. Maiya, to be published.

[6] Conway, J. B., Berling, J. T., and Stentz, R. H., "A New Correlation of the Effects of Hold Time on Low-cycle Fatigue Behavior," GEMP-702, (General Electric Company, June 1969).

[7] Diercks, D. R. and Raske, D. T., "Elevated-temperature Strain-controlled Fatigue Data on Type 304 Stainless Steel: A Compilation, Multiple Linear Regression Model, and Statistical Analysis, ANL-76-95 (Argonne National Laboratory, December 1976).

[8] Cheng, C. Y. and Diercks, D. R., "Effects of Hold Time on Low-cycle Fatigue Behavior of AISI Type 304 Stainless Steel at 593°C," Metallurgical Transactions, Vol. 4, No. 2, 1973, pp. 615-617.

[9] Maiya, P. S. and Majumdar, S., "Application of Frequency-Modified Life Approach to the Low-cycle Fatigue Behavior of Type 304 Stainless Steel," ANL-76-40 (Argonne National Laboratory, May 1976).

[10] Gittus, J., "Theory of Fatigue Failure of Cavity Formation," in *Thermal and High-Strain Fatigue* (The Metals and Metallurgy Trust of the Institute of Metals and the Institution of Metallurgists, London, 1967), p. 142.

[11] Tomkins, B. and Wareing, J., *Elevated Temperature Fatigue Interactions in Engineering Materials*, TRG Report 3003 (s) (United Kingdom Atomic Energy Authority, London, March 1977).

[12] Raj, R., "Time Dependent Effect in Creep-Fatigue," in *1976 ASME-MPC Symposium on Creep-Fatigue Interaction*, MPC-3 (American Society of Mechanical Engineers, New York, 1976), pp. 337-348.

[13] Majumdar, S. and Maiya, P. S., "A Unified and Mechanistic Approach to Creep-Fatigue Damage," in *Proceedings of the Second International Conference on Mechanical Behavior of Materials*, ICM-II (American Society for Metals, Metals Park, Ohio, 1976), p. 924-928. See also ANL-76-58 (Argonne National Laboratory, January 1976).

[14] Hart, E. W., "A Phenomenological Theory for Plastic Deformation of Polycrystalline Metal," Acta. Metallurgica, Vol. 18, 1970, p. 599.

[15] Majumdar, S. and Maiya, P. S., "Wave-shape Effects in Elevated-temperature Low-cycle Fatigue of Type 304 Stainless Steel," presented at the ASME/CSME Pressure Vessel and Piping Conference to be held in Montreal, Canada, June 25-29, 1978.

[16] Slot, T., Stentz, R. H., and Berling, J. T., "Controlled-strain Testing Procedures," in *Manual on Low-cycle Fatigue Testing*, ASTM STP 465 (American Society for Testing and Materials, Philadelphia, 1969), p. 100.

[17] Majumdar, S. and Maiya, P. S., "Hold-time-sequence Effects on the Elevated-temperature Low-cycle Fatigue of Type 304 Stainless Steel," to be presented at the Winter Annual Meeting of the American Society of Mechanical Engineers, San Francisco, California, December 1978.

[18] Majumdar, S. and Maiya, P. S., "A Damage Equation for Creep-Fatigue Interaction," in *1976 Symposium on Creep-Fatigue Interaction*, MPC-3 (American Society of Mechanical Engineers, New York, 1976), pp. 323-335.

[19] Machlin, E. S., Discussion of Paper, "Mechanisms of Intergranular Fracture at Elevated Temperatures," by Gifkins, R. C., in *Fracture* (Technology Press of Massachusetts Institute of Technology, Cambridge, Mass., 1959), pp. 623-626.

Table I. Effects of Wave Shape on the Fatigue Life of Type 304 Stainless Steel at 593°C (1100°F).

Specimen No.	$\Delta\varepsilon_t$ (%)	$\Delta\varepsilon_p$ (%)	$\Delta\sigma$ (MPa)	Tens. $\dot{\varepsilon}_t$ (s^{-1})	Comp. $\dot{\varepsilon}_t$ (s^{-1})	t_t (min)	t_c (min)	N_f (cycles)	Type of Test
T-389	1.00	0.67	494.0	1×10^{-4}	1×10^{-4}	0	0	1697	Slow-slow
T-467	1.00	0.69	464.7	1×10^{-4}	1×10^{-2}	0	0	847	Slow-fast
T-468	1.00	0.68	479.1	1×10^{-2}	1×10^{-4}	0	0	3025	Fast-slow
T-320	1.01	0.70	473.0	4×10^{-2}	4×10^{-2}	0	0	5096	Fast-fast
T-85	1.01	0.73	422.0	4×10^{-6}	4×10^{-6}	0	0	579	Slow-slow
T-462	1.00	0.72	428.0	4×10^{-6}	4×10^{-3}	0	0	261	Slow-fast
T-465	0.99	0.69	451.6	4×10^{-3}	4×10^{-6}	0	0	2421	Fast-slow
T-35	1.00	0.66	518.0	4×10^{-3}	4×10^{-3}	0	0	3395	Fast-fast
T-431	0.99	0.74	427.2	4×10^{-3}	4×10^{-3}	10	10	2507	Symmetrical hold
T-472	1.01	0.77	417.6	4×10^{-3}	4×10^{-3}	15	5	1788	Unsymmetrical hold
T-30	1.00	0.74	441.0	4×10^{-3}	4×10^{-3}	15	0	666	Tensile hold
T-44	2.00	1.66	605.0	4×10^{-3}	4×10^{-3}	15	0	237	Tensile hold
T-475	2.00	1.74	571.5	4×10^{-3}	4×10^{-3}	15	5	642	Unsymmetrical hold

Table II. Stress-relaxation Parameters[a] for Type 304 Stainless Steel at 593°C (1100°F).

Specimen No.	Tension				Compression			
	Hold Time (min)	σ_i (MPa)	B	p	Hold Time (min)	σ_i (MPa)	B	p
T-431	10	213.6	0.045	-0.725	10	213.6	0.043	-0.717
T-472	15	217.3	0.055	-0.826	5	200.3	0.084	-0.677
T-30	15	218.4	0.017	-0.881	0	222.6	-	-
T-44	15	304.2	0.031	-0.833	0	300.8	-	-
T-475	15	298.5	0.040	-0.854	5	273.0	0.052	-0.786

[a]Determined from Eq. (11), with t in minutes.

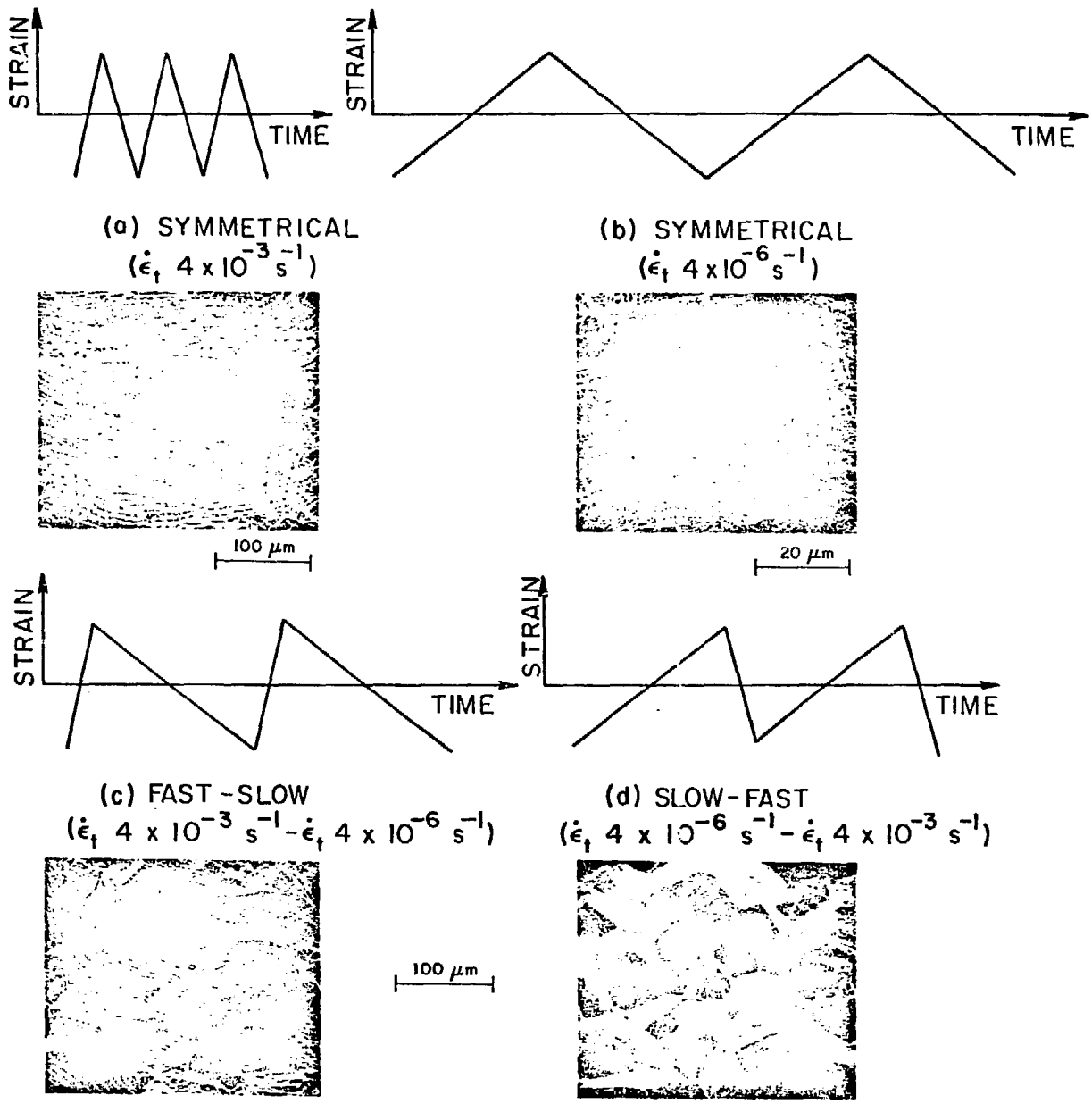

Fig. 1. Effect of wave shape on fatigue-fracture surface appearance ($\dot{\epsilon}_f$ = 4 x 10^{-3} s^{-1} and $\dot{\epsilon}_s$ = 4 x 10^{-6} s^{-1}).

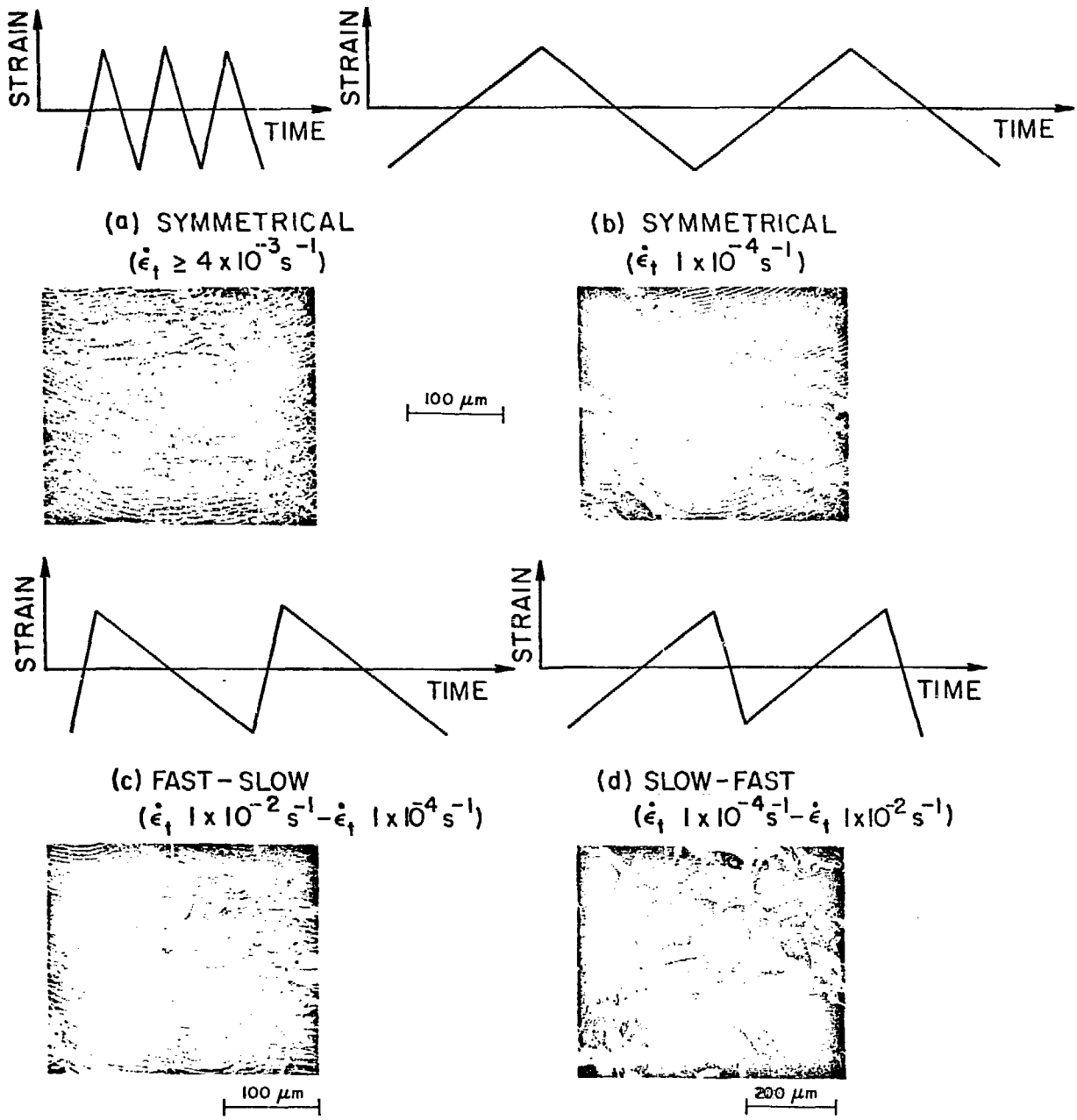

Fig. 2. Effect of wave shape on fatigue-fracture surface appearance ($\dot{\epsilon}_f = 1 \times 10^{-2}$ s^{-1} and $\dot{\epsilon}_s = 1 \times 10^{-4}$ s^{-1}).

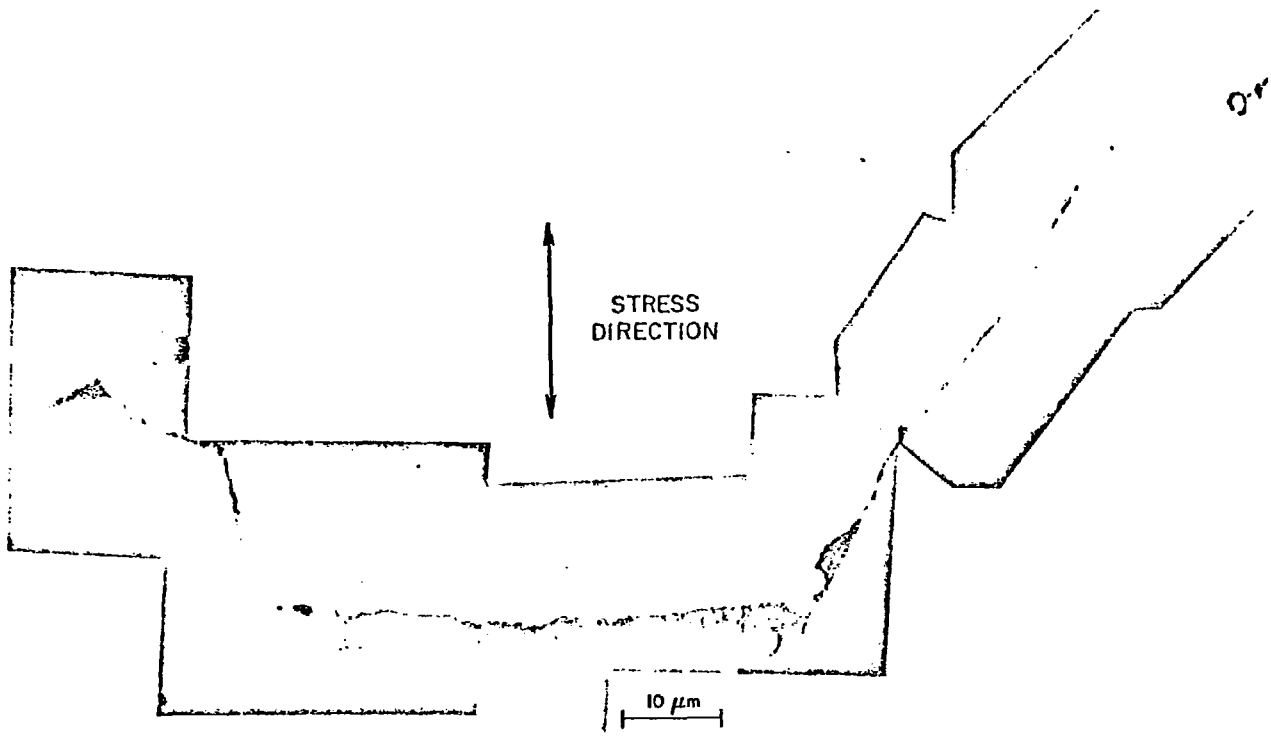

Fig. 3. Scanning-electron micrograph showing grain-boundary cavities in specimen T462.

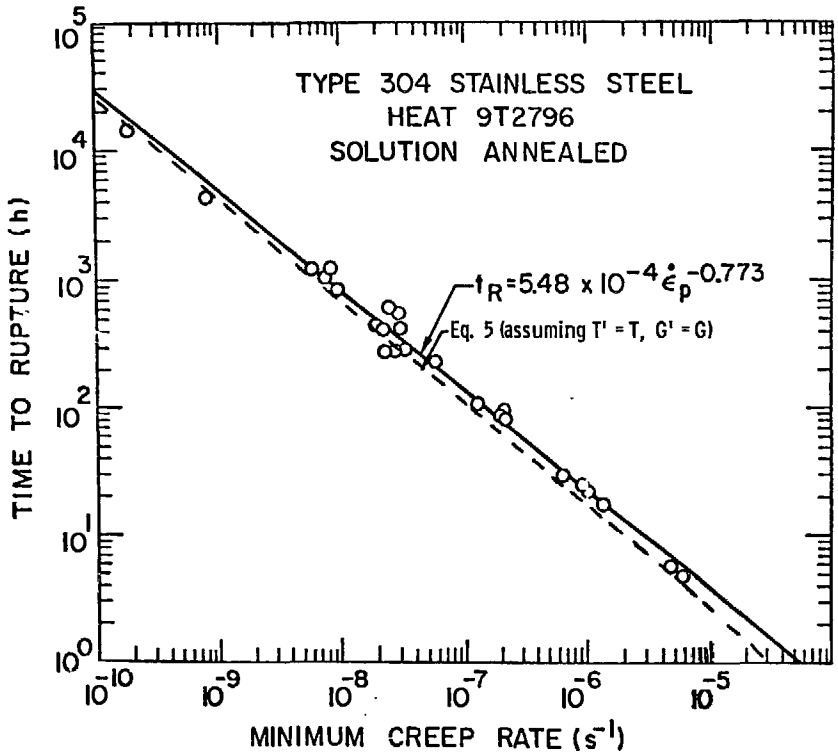

Fig. 4. Time-to-rupture vs minimum creep rate for Type 304 stainless steel at 593°C (1100°F).

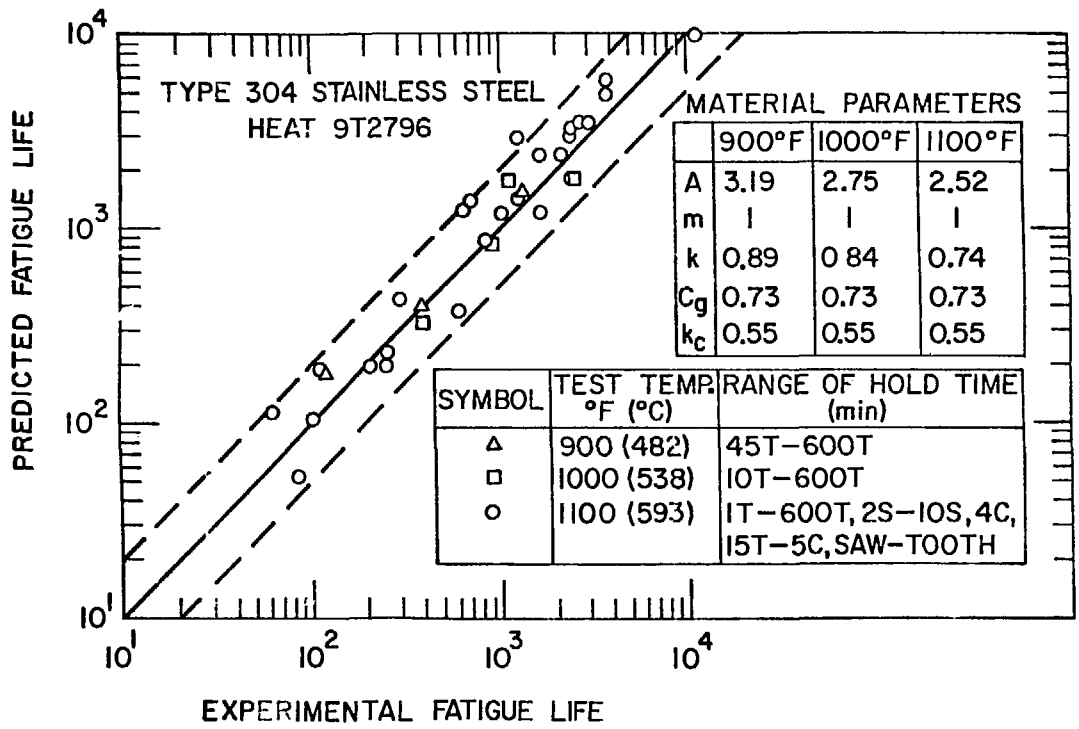

Fig. 5. Comparison of experimentally observed and predicted fatigue lives for Type 304 stainless steel under loadings of various waveforms.